Investigation of fundamental mechanisms related to ambient gas heating and hydrodynamics of laser-induced plasmas

P. J. Skrodzki

Acknowledgements

This work is supported by the DOE/NNSA Office of Nonproliferation and Verification Research and Development (NA-22). Pacific Northwest National Laboratory is operated for the U.S. DOE by the Battelle Memorial Institute under Contract No. DE-AC05-76RLO1830. P. J. Skrodzki and A. Miloshevsky would like to acknowledge support and funding from Summer Undergraduate Laboratory Internship program sponsored by the U.S. DOE.

People

S. S. Harilal

M. C. Phillips

A. Miloshevsky

B. E. Brumfield

N. L. LaHaye

K. C. Hartig

I. Jovanovic

N. P. Shah

N. Taylor

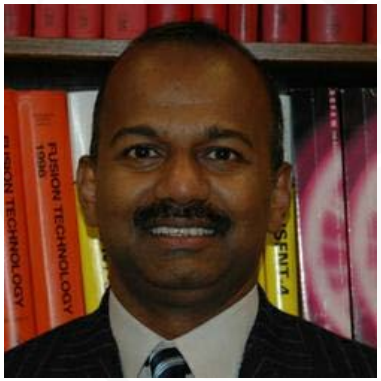

Pacific Northwest NATIONAL LABORATORY

Laser-induced plasmas (LIP)

- Remote sensing applications [1-2]:
  - Nuclear safeguards
  - Space exploration
  - Biological/geological forensics

Mars Curiosity Rover

- Intense pulsed laser focused onto a target generates plasma
  - Plasma consists of excited atoms, ions, molecules, nano- and micro-particles
  - Plasma cools emitting electromagnetic radiation
    - Emission useful as diagnostic tool through spectroscopy

[1] J. P. Singh and S. N. Thakur, Laser Induced Breakdown Spectroscopy (Elsevier, Amsterdam, 2007).
[2] S. Musazzi and U. Perini, Laser-Induced Breakdown Spectroscopy—Fundamentals and Applications (Springer Series in Optical Sciences, 2014).

Optical sensing techniques

1. Laser-ablation (LA) coupled with optical emission spectroscopy (OES)
2. LA molecular isotopic spectrometry (LAMIS)
3. LA coupled with laser absorption spectroscopy (LAS)
4. Various imaging techniques (i.e. spectral mapping, shadowgraphy)

Typical Emission Spectroscopy Schematic

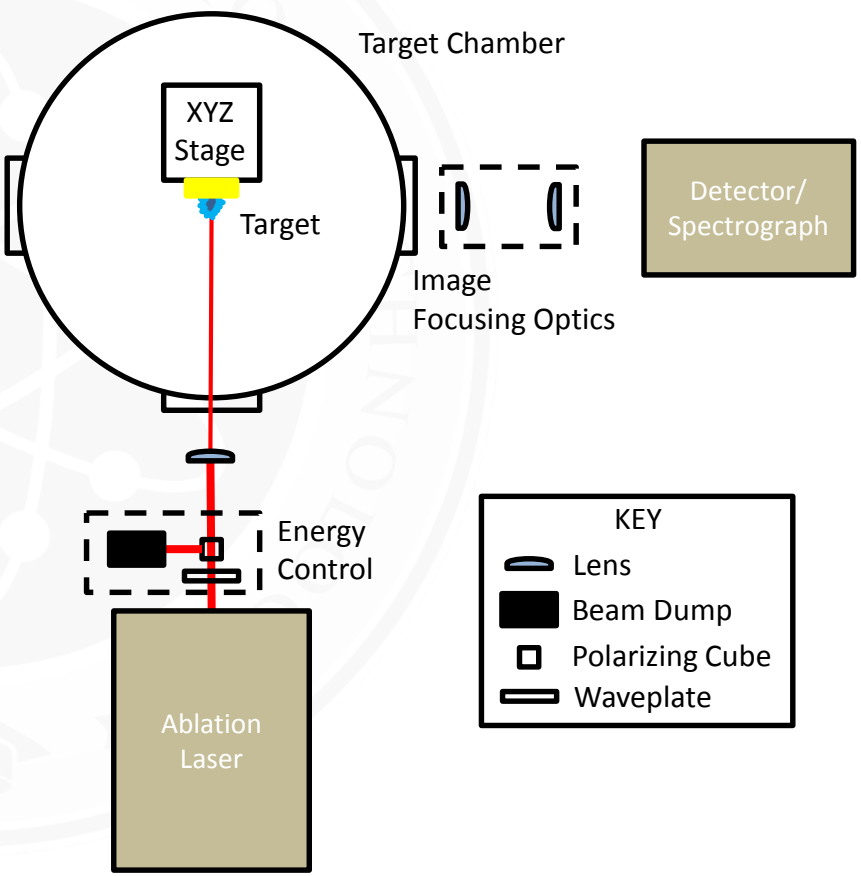

LIP for nuclear material sensing

LIP related techniques for nuclear material sensing	
Advantages	**Disadvantages**
Non-destructive spectroscopic methods	Matrix effects from multi-element targets
Remote detection capability	Congested spectra from high-Z targets (Th, U, Pu)
High spatial (µm) and temporal (<fs) resolution	Limited studies/models for molecular Th, U, Pu
Vast parametric space for signal optimization	Material detection/ID vs. radiation detection

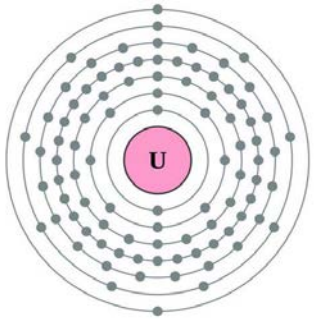

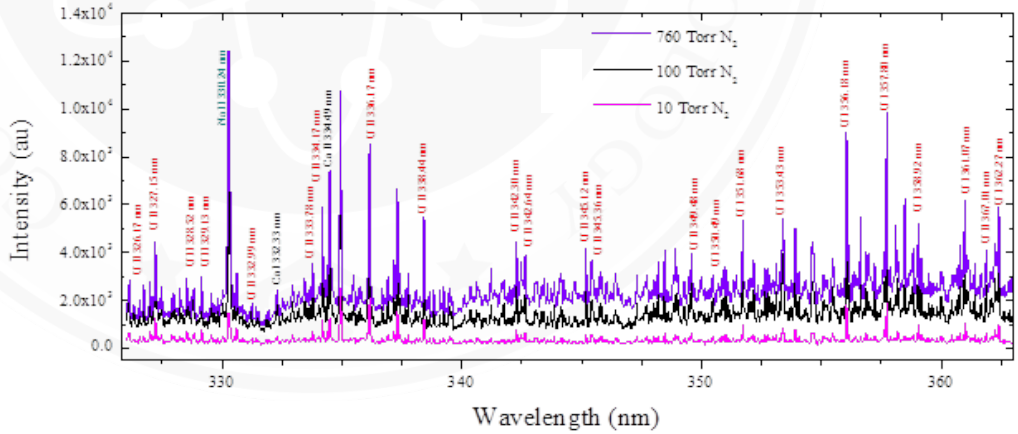

Skrodzki *et al*. (2016)

LIP for nuclear material sensing

Vast parametric space for optimization

↑Precision; Isotope distinction

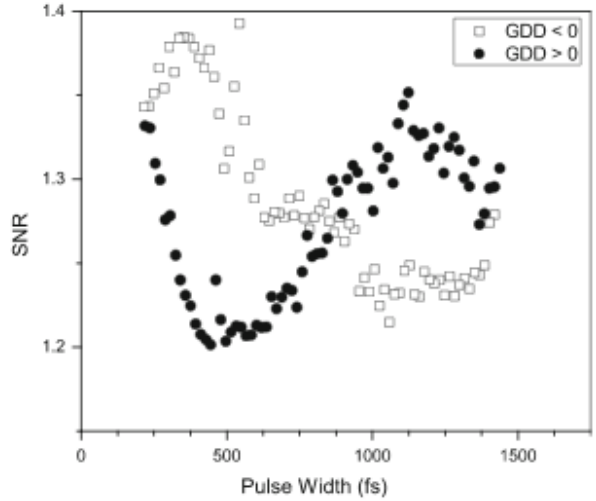

Hartig *et al.* (2013)

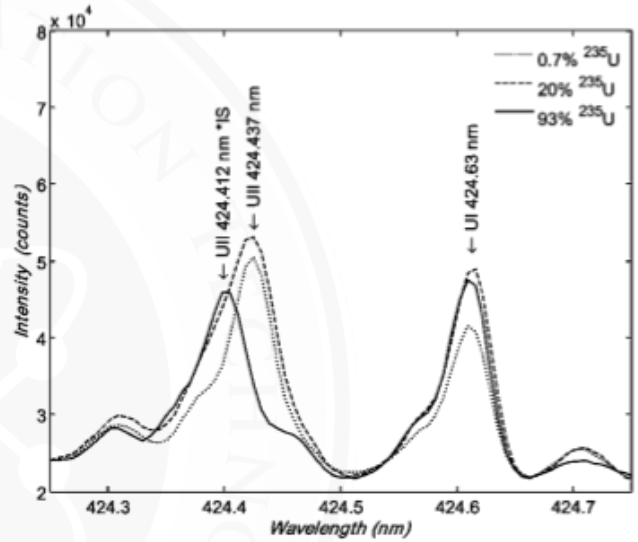

Doucet *et al.* (2011)

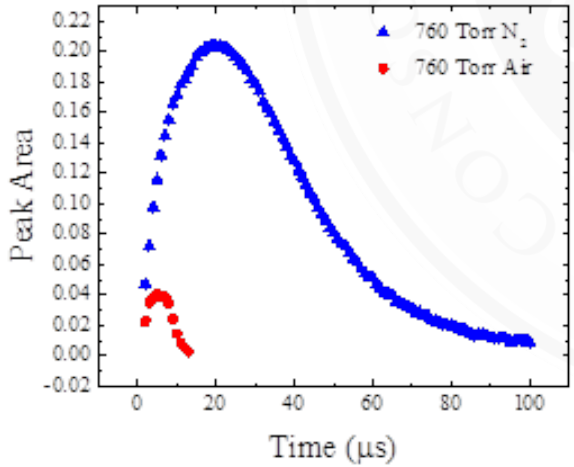

Skrodzki *et al.* (2016)

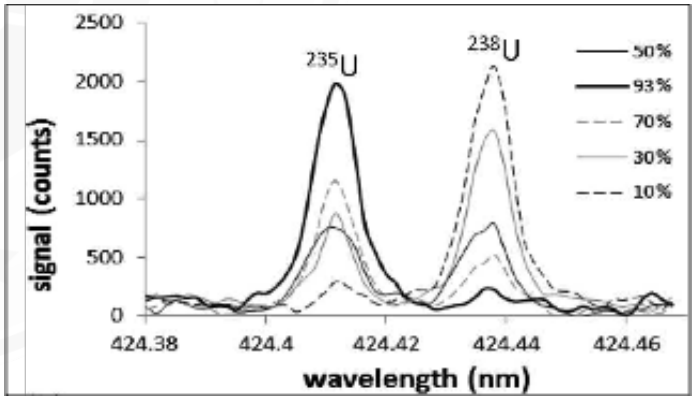

Cremers *et al.* (2012)

Recent LIP applications in U sensing

- Dual-pulse (DP) OES enhances standard single-pulse (SP) signal
- Initial pulse ablates target
- Secondary pulse reheats plasma → more emission
- Also increases background and noise

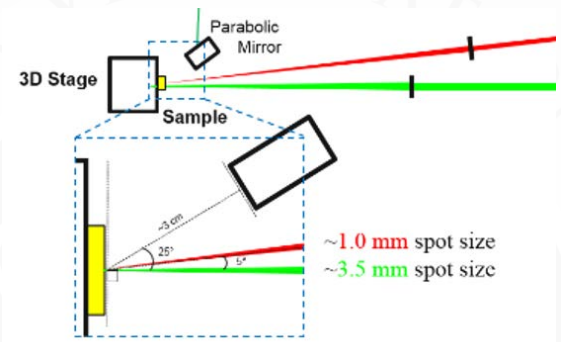

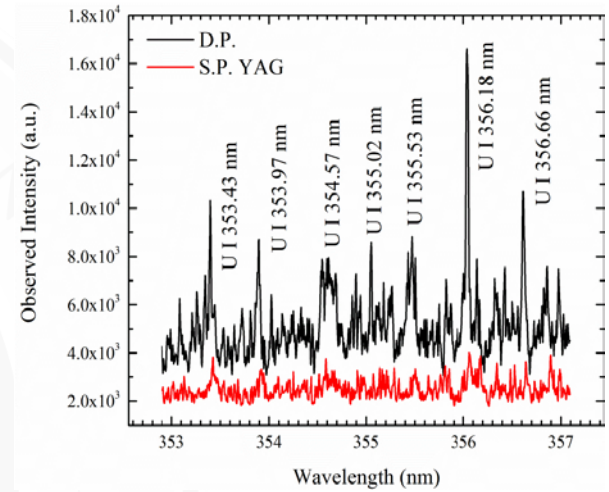

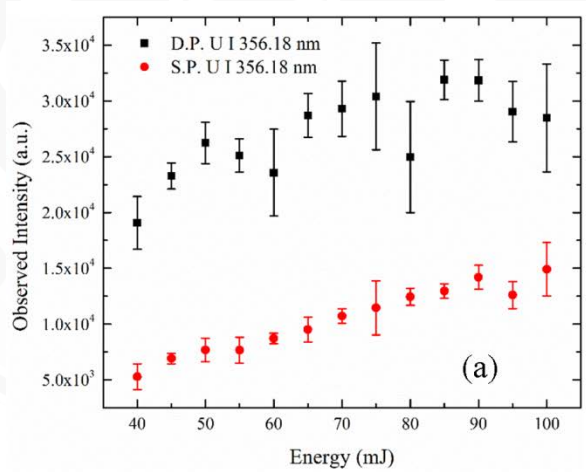

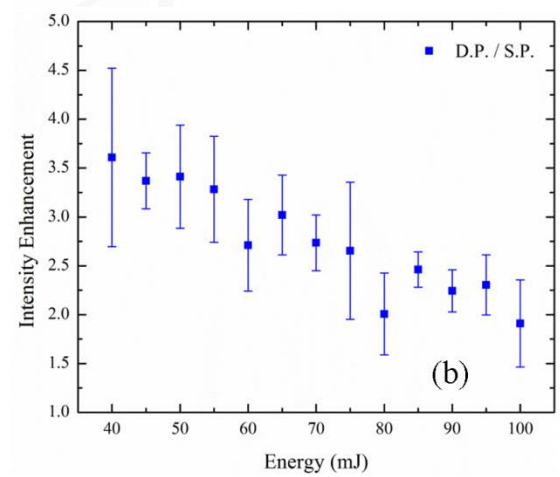

[3] P. J. Skrodzki, J. R. Becker, P. K. Diwakar, S. S. Harilal, A. Hassanein, Applied Spectroscopy (2016).

Recent LIP applications in U sensing

- Recent comparison of U emission spectra from two solid targets [4]:
  - Kopp glass containing 1.3% natural U by mass
  - Depleted U metal
- U oxide bands prevalent among several U I features in metal
- Matrix effects mitigate U signal in glass

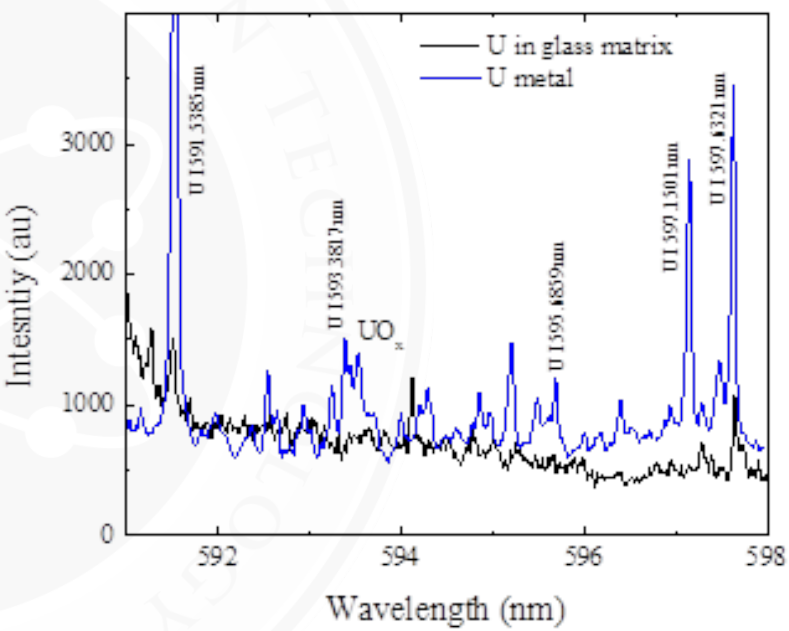

[4] P. J. Skrodzki, N. P. Shah, N. Taylor, K. C. Hartig, N. L. LaHaye, B. E. Brumfield, I. Jovanovic, M. C. Phillips, S. S. Harilal , Spectrochimica Acta B (2016).

Laser-induced sparks & impetus

- Aforementioned studies include primarily solid targets
- Gaseous targets generate *sparks* which have various applications in ignition, machining, further nuclear material sensing
- Uranyl fluoride (UO_2F_2) is relevant to enrichment process and may be an indicator of enrichment facilities

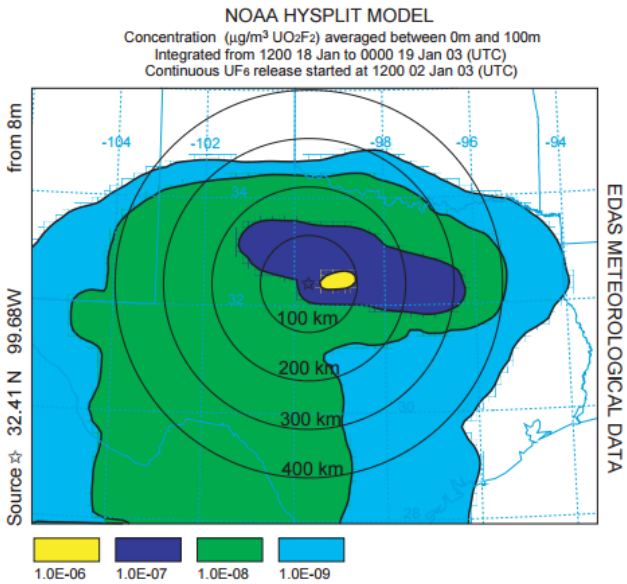

Fig. 2. Isopleths for routine-release. UO_2F_2 concentration in $\mu g/m^3$.

Kemp (2006)

Impetus

1. Employ optical sensing and imaging techniques to understand spark morphology
2. Identify physical phenomena associated with expansion and collapse of sparks
3. Optimize spectroscopic viewing windows (spatial and temporal) in sparks for latter applications in UO_2F_2 sensing

Expansion & collapse of sparks

Previous literature shows heating (excitation and ionization) of the gas surrounding the spark [5]:

1. Prompt electrons:
   - Originate from interaction between laser pulse and target
   - ~10^1-10^2 ns
2. Radiative heating:
   - Intense ultraviolet (UV) radiation from plasma
   - Early emission (~10^1-10^3 ns) relative to plasma lifetime (~ms)
   - Instantaneous interaction with surrounding gas
3. Detonative heating
   - Pressure/density gradient from LPP generates shock
   - Shock expands detaching from plasma (~10^1-10^2 µs)

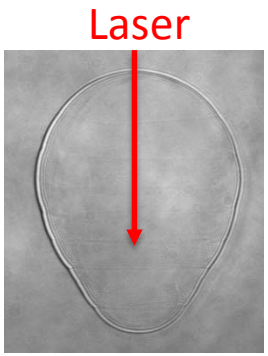

Air Shockwave (400 ns)

[5] S. S. Harilal, B. E. Brumfield, and M. C. Phillips, "Lifecycle of laser-produced air sparks," Phys. Plasmas 22, 063301 (2015).

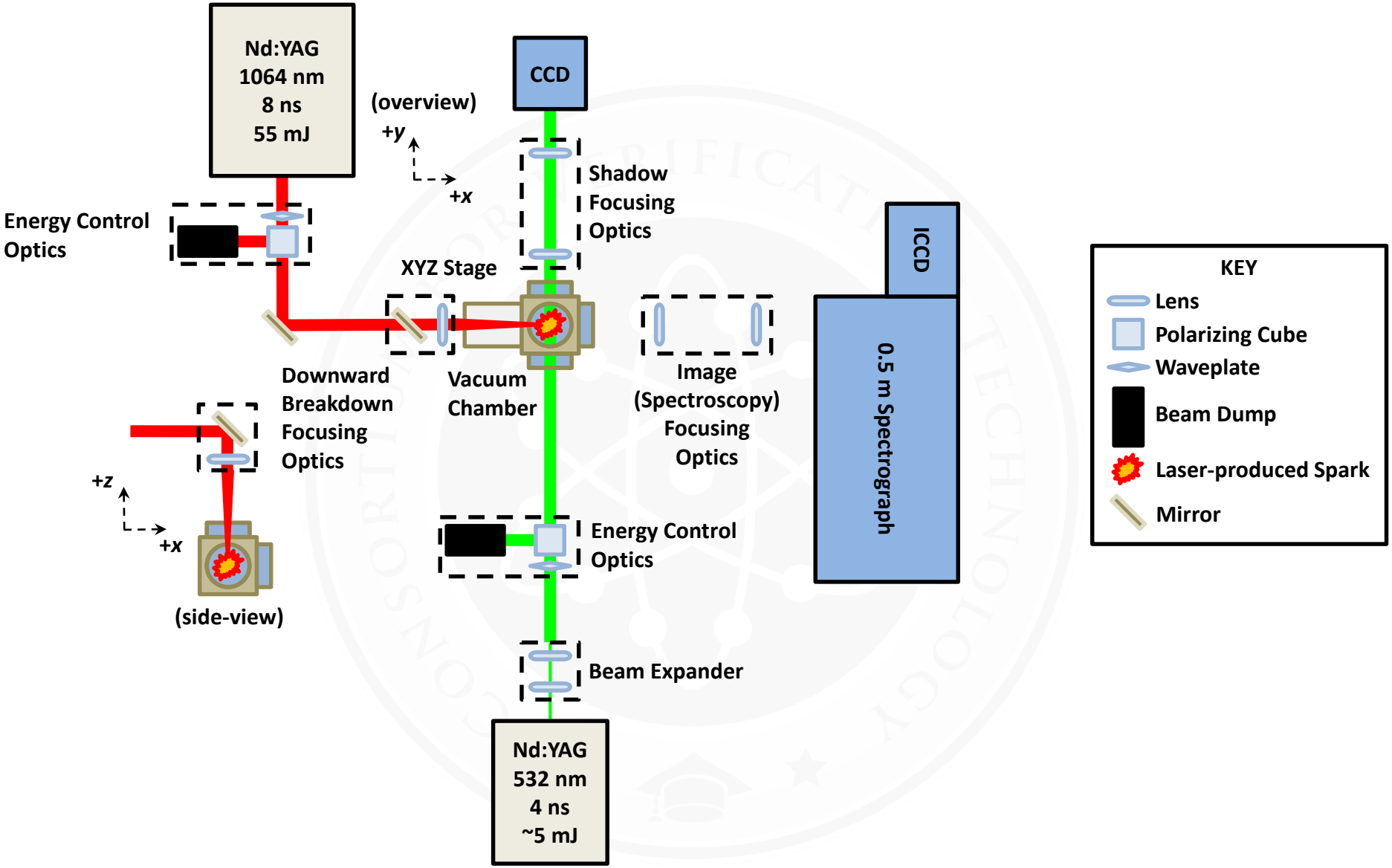
Nd:YAG
1064 nm
8 ns
55 mJ
(overview)
+y
+x
CCD
Shadow
Focusing
Optics
Energy Control
Optics
XYZ Stage
ICCD
0.5 m Spectrograph
Downward
Breakdown
Focusing
Optics
Vacuum
Chamber
Image
(Spectroscopy)
Focusing
Optics
+z
+x
(side-view)
Energy Control
Optics
Beam Expander
Nd:YAG
532 nm
4 ns
~5 mJ
KEY
Lens
Polarizing Cube
Waveplate
Beam Dump
Laser-produced Spark
Mirror

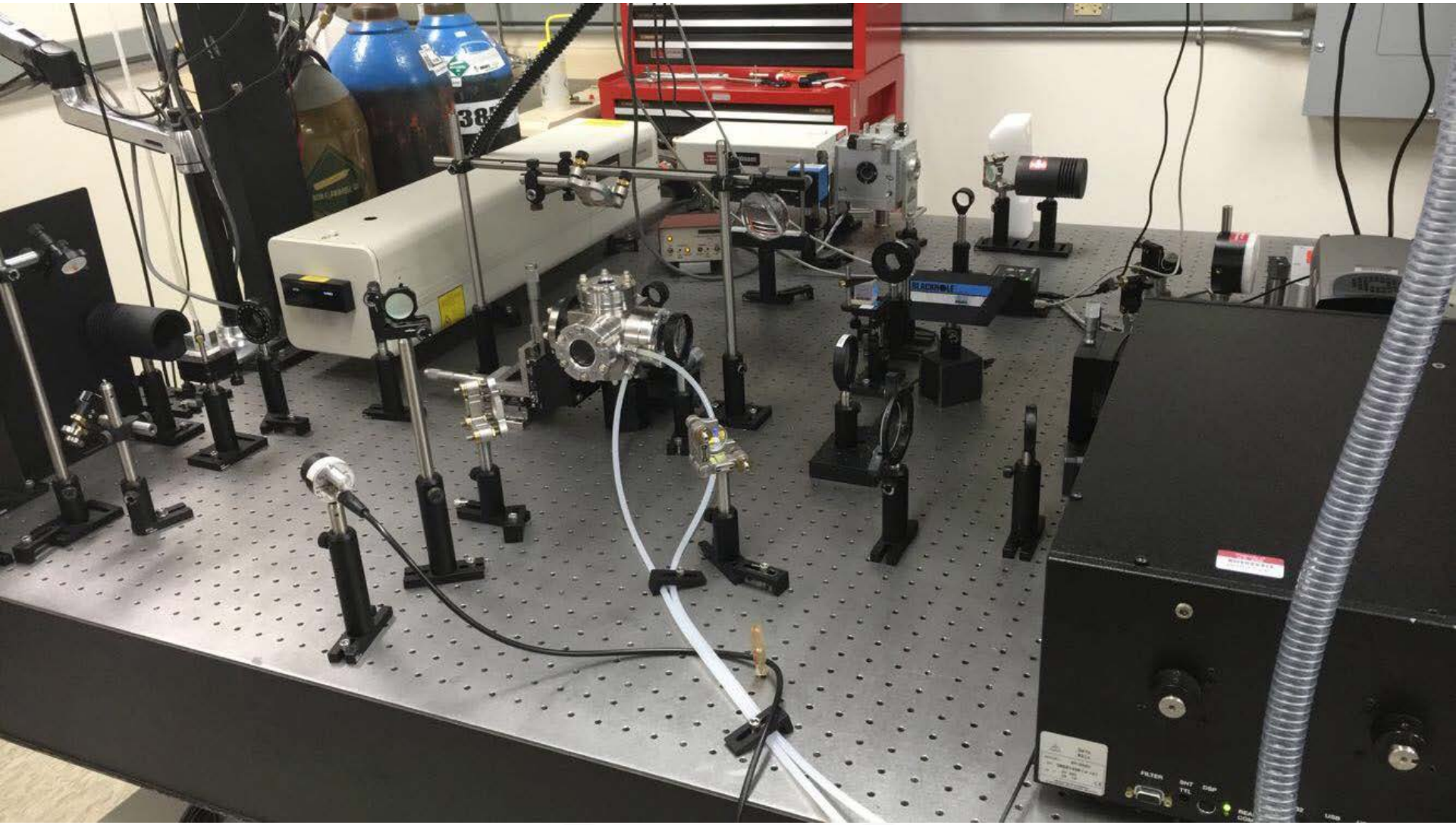

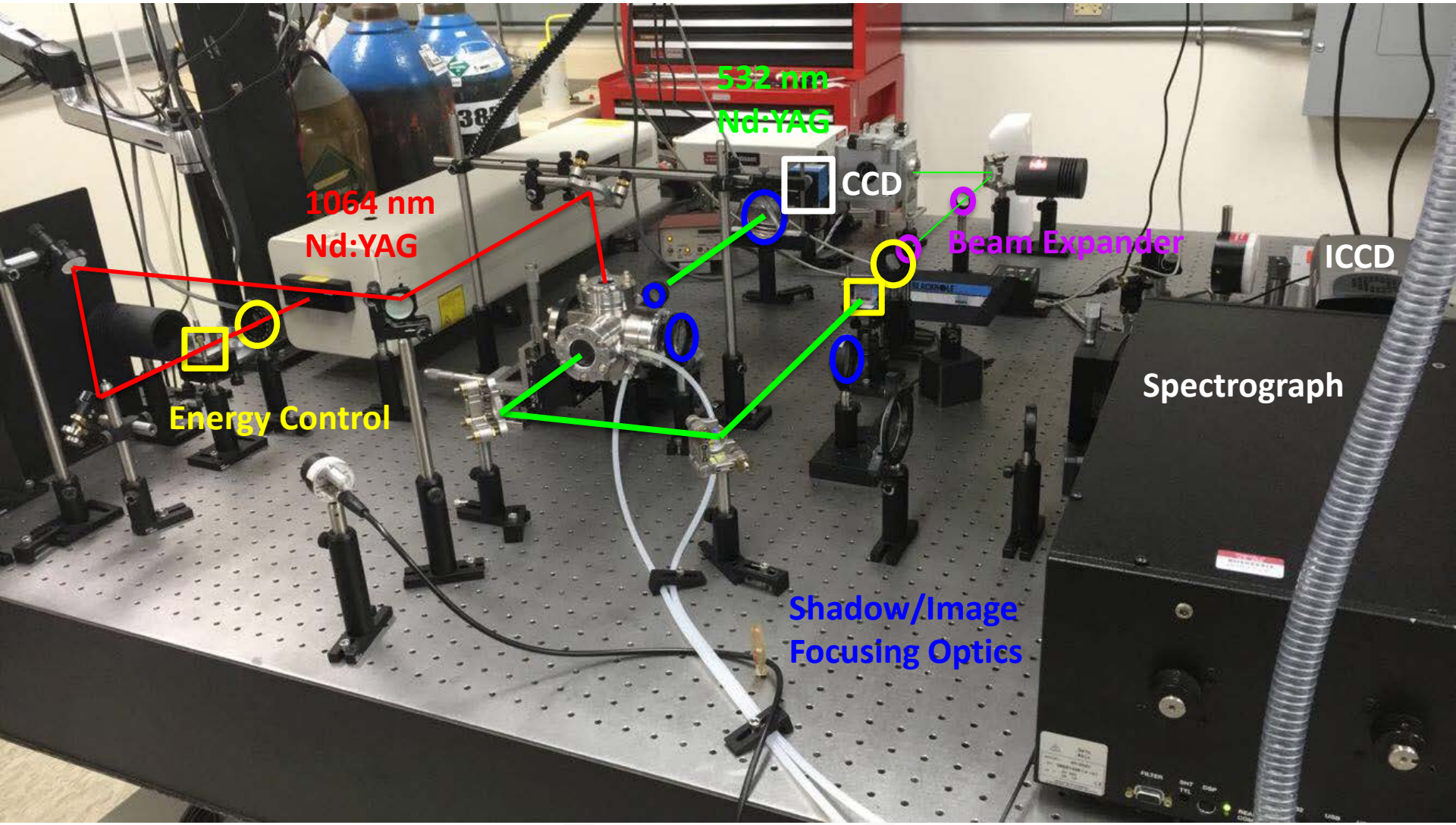
532 nm
Nd:YAG
CCD
1064 nm
Nd:YAG
Beam Expander
ICCD
Spectrograph
Energy Control
Shadow/Image
Focusing Optics

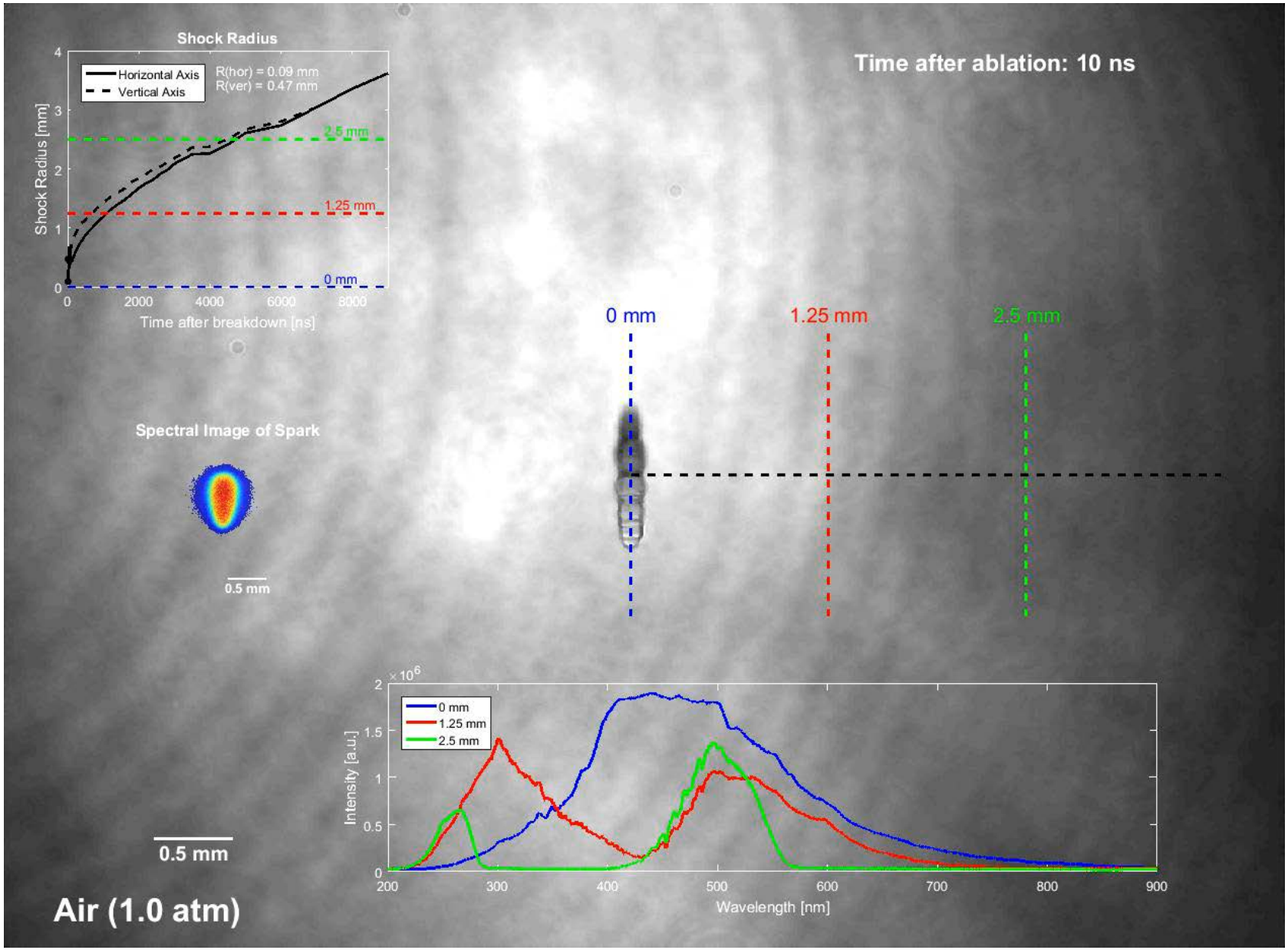
Shock Radius
Horizontal Axis
Vertical Axis
R(hor) = 0.09 mm
R(ver) = 0.47 mm
2.5 mm
1.25 mm
0 mm
Shock Radius [mm]
Time after breakdown [ns]
Time after ablation: 10 ns
0 mm
1.25 mm
2.5 mm
Spectral Image of Spark
0.5 mm
0 mm
1.25 mm
2.5 mm
Intensity [a.u.]
Wavelength [nm]
0.5 mm
Air (1.0 atm)

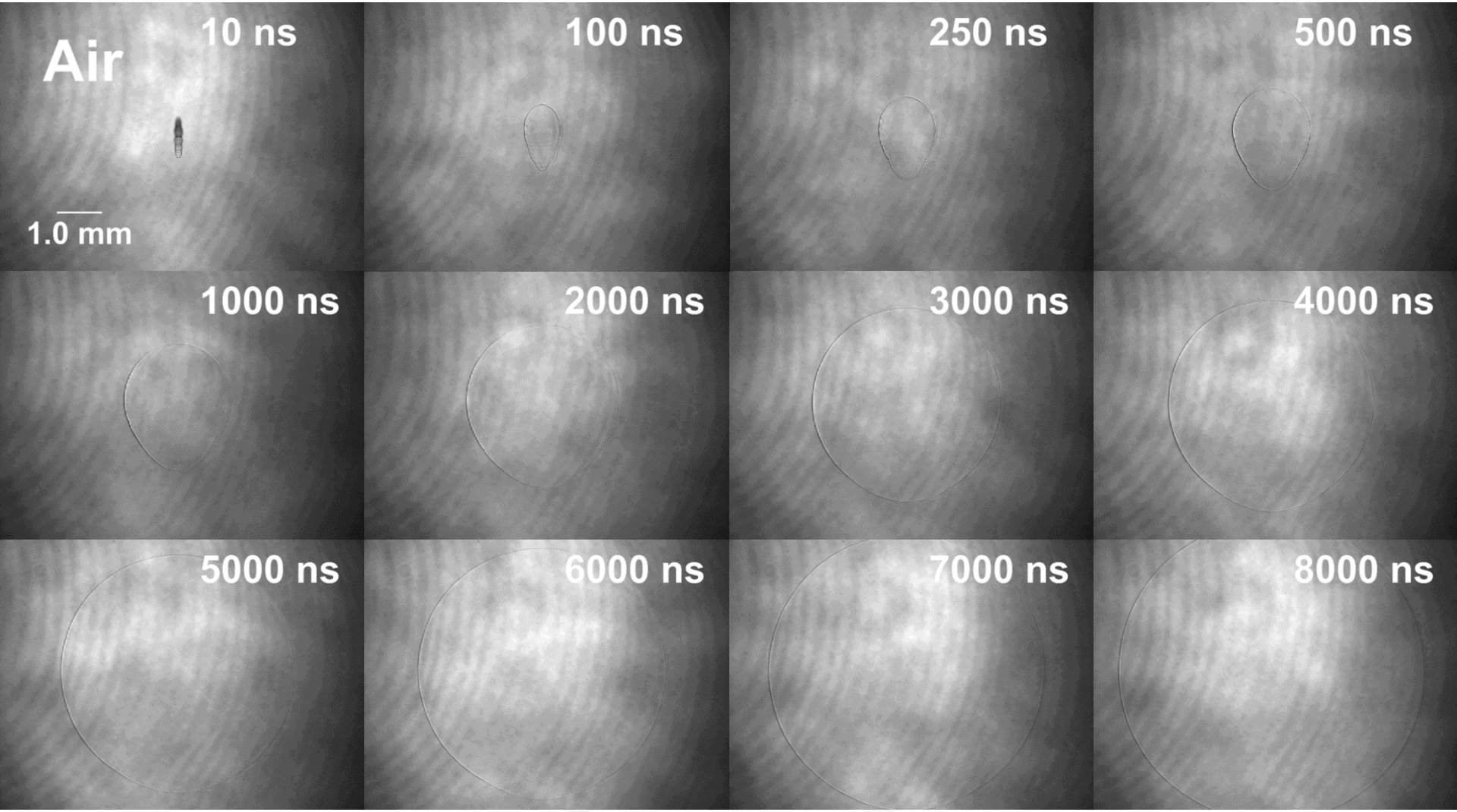
Air
10 ns
1.0 mm
100 ns
250 ns
500 ns
1000 ns
2000 ns
3000 ns
4000 ns
5000 ns
6000 ns
7000 ns
8000 ns

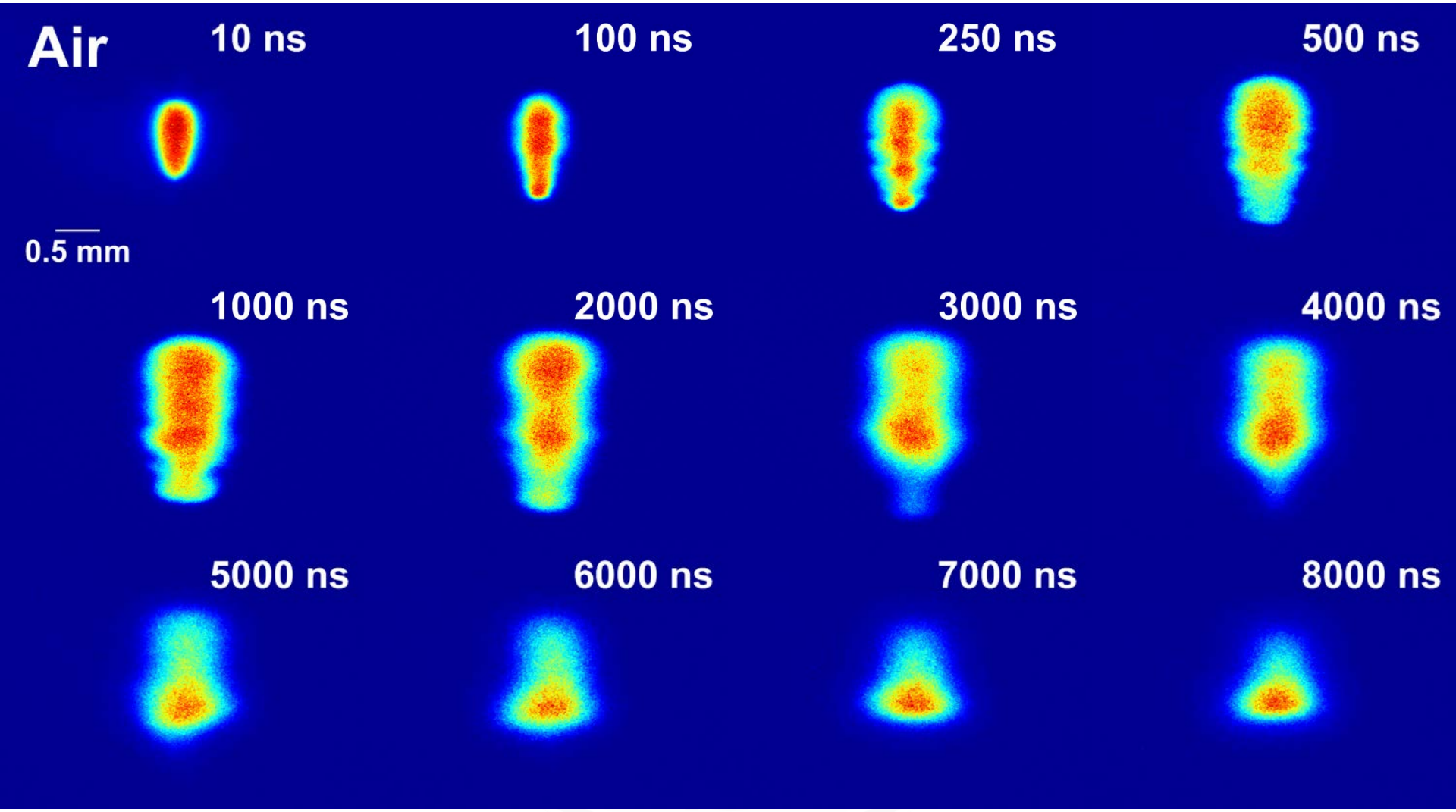
Air
10 ns
100 ns
250 ns
500 ns
0.5 mm
1000 ns
2000 ns
3000 ns
4000 ns
5000 ns
6000 ns
7000 ns
8000 ns

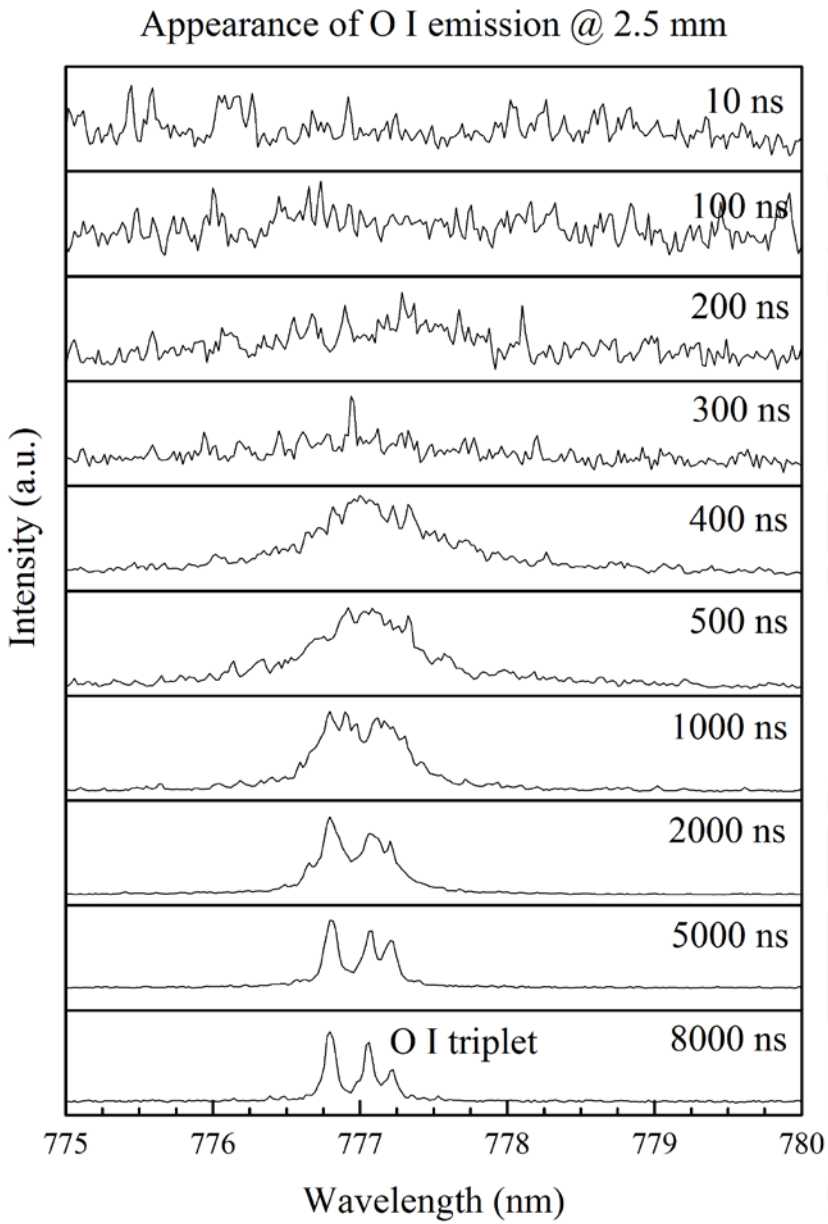

- Appearance of O I emission features at ~300-400 ns at 2.5-mm distance from kernel
- Shock only reaches 2.5-mm distance after 4500 ns
- Profound late-time features following arrival of plasma

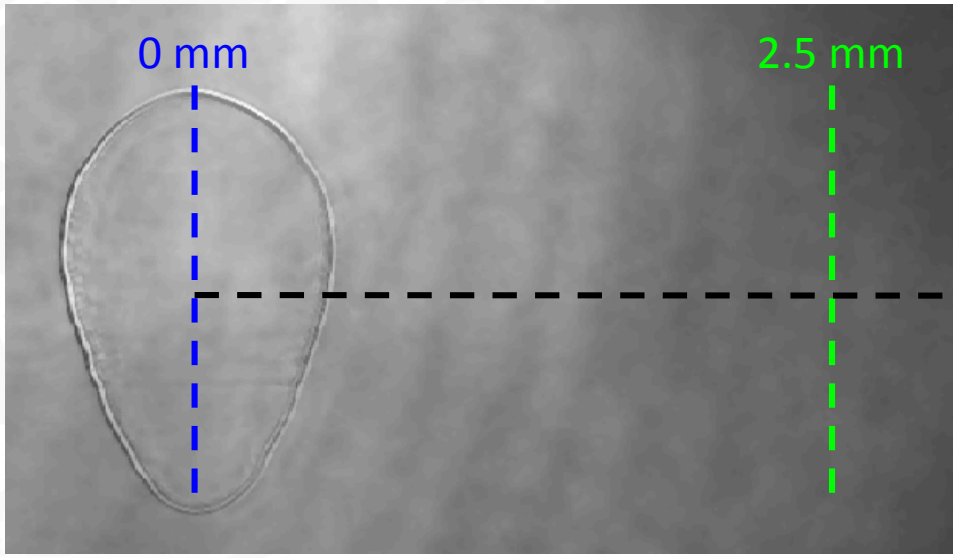

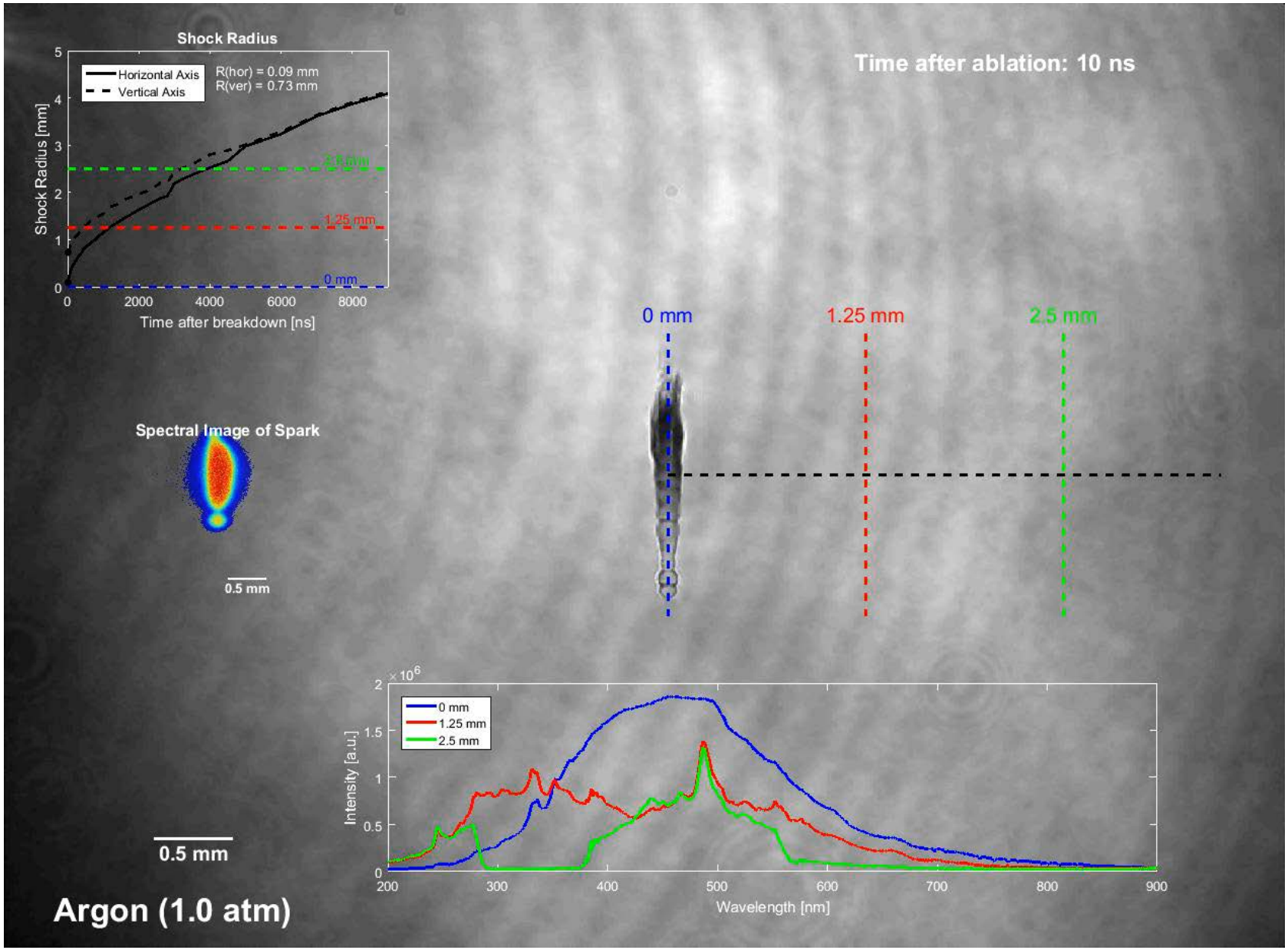
Shock Radius
Horizontal Axis
Vertical Axis
R(hor) = 0.09 mm
R(ver) = 0.73 mm
Shock Radius [mm]
Time after breakdown [ns]
2.5 mm
1.25 mm
0 mm
Time after ablation: 10 ns
0 mm
1.25 mm
2.5 mm
Spectral Image of Spark
0.5 mm
0.5 mm
Argon (1.0 atm)
Intensity [a.u.]
Wavelength [nm]
0 mm
1.25 mm
2.5 mm

Modeling Details

Model

- Open source Computational Fluid Dynamics (CFD) software package OpenFOAM
- 2D numerical simulation of laser-induced electrical breakdown of air
- Computational domain: 5-mm (*x*-axis) x 10-mm (*y*-axis) discretized into 250 x 500 cell mesh, respectively
- Left-side *y*-boundary considered a symmetry axis while outflow boundaries are placed sufficiently far from region of interest in flow field

Parameter Space

- Ambient: Ar; pressure 101,325 kPa; temperature 300 K
- Initial plasma specified as ellipse with 50-µm (*x*-axis) x 150-µm (*y*-axis) major axis lengths
- Initial plasma: air; pressure 25 MPa; temperature 70,000 K
- Equation of state: Ideal Gas Law
- Duration: 10 µs following onset of laser pulse

Pressure Contours

Temperature Contours

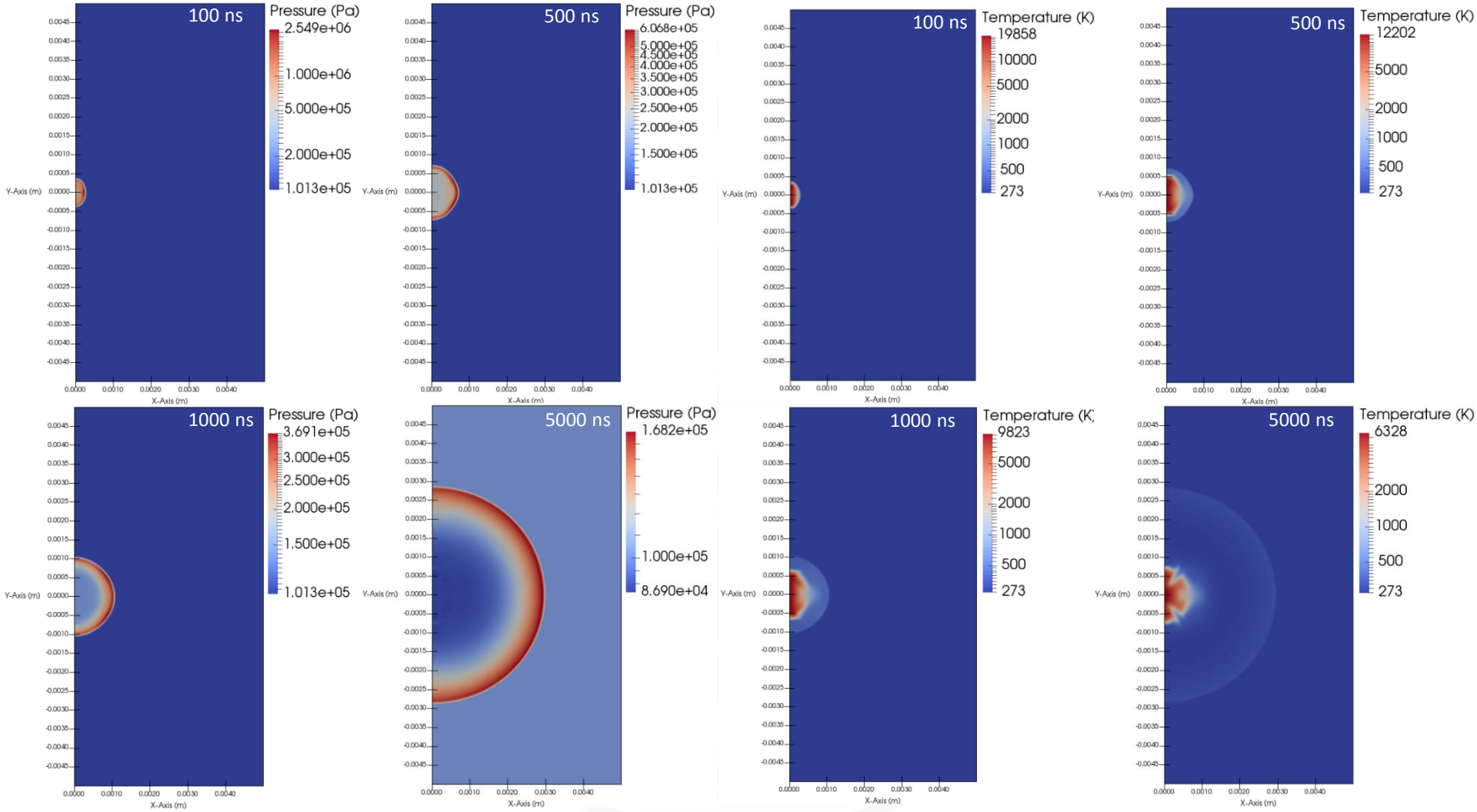

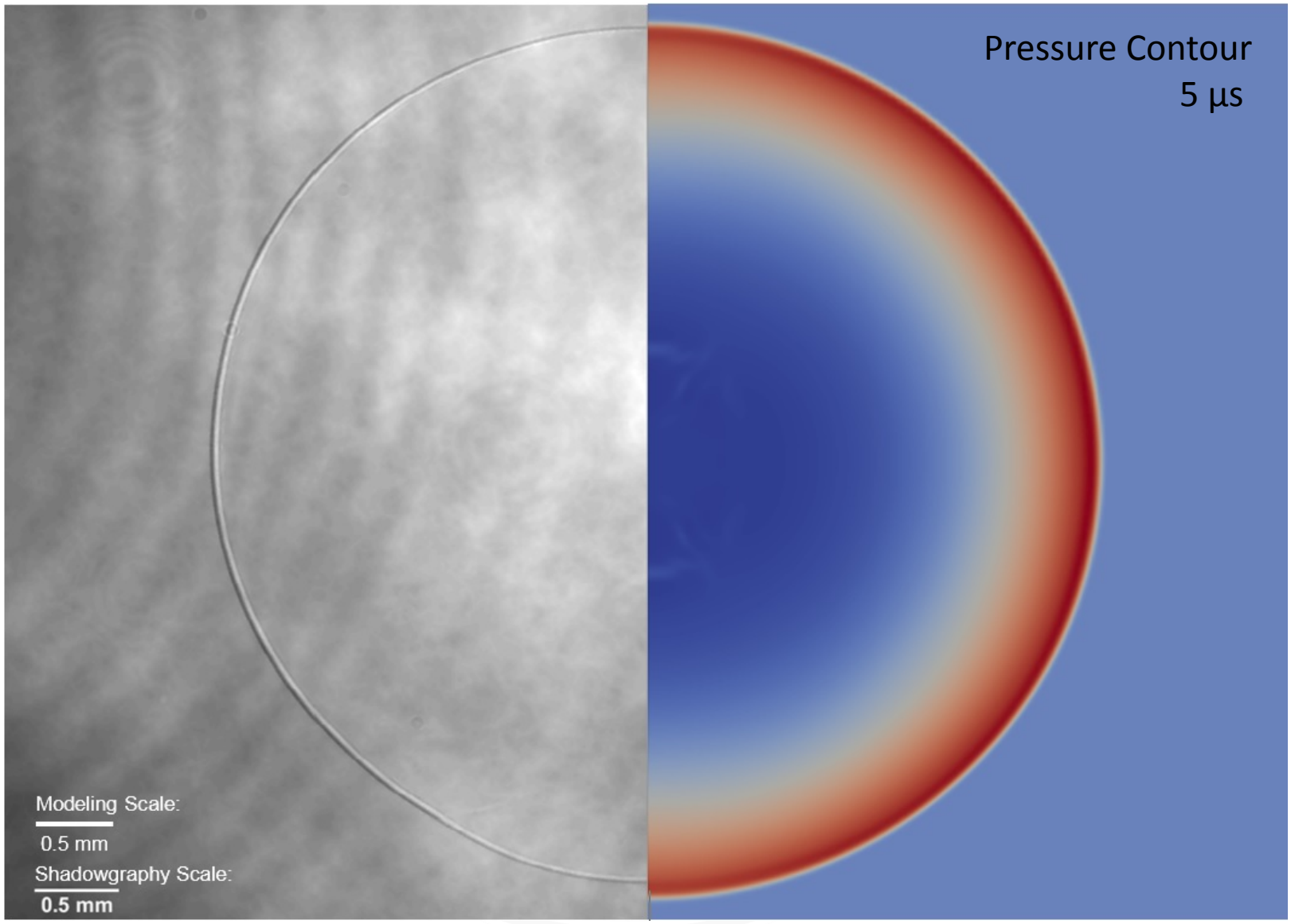
Pressure Contour
5 µs
Modeling Scale:
0.5 mm
Shadowgraphy Scale:
0.5 mm

Conclusion & future work

Experiment

- Different gases exhibit unique shock morphologies related to laser absorption parameters
- Observed time-dependent emission features unique to each gas
  - Broad mixing at early times, ionic emission, neutral emission, then molecular emission
- Radiative heating proves dominant mechanism; detonative heating negligible

Model

- The shockwave pressure is ~20 times greater than the atmospheric pressure at 100 ns and then rapidly decreases as the spark decays
- The shock front becomes increasingly symmetric in the shape with time
- The temperature of the plasma has severely decreased from 70,000 K to ~20,000 K during the first 100 ns

Future Work

- Expanding optical techniques to sparks containing UO_2F_2

Experiment Details

Breakdown

- Generate gaseous spark in four gases (air, argon, nitrogen, helium) at atmospheric pressure (~760 Torr)
- 55 mJ energy, 1064 nm Nd:YAG (8 ns FWHM) focused to ~100 µm spot diameter – 90 GW cm^{-2}

Time-resolved Shadowgraphy

- Pressure/density difference along shock-front has different refractive index
- Observe shock by shining backlight laser through spark onto CCD camera
- ~5 mJ, 532 nm Nd:YAG (4 ns FWHM) expanded to ~1 cm spot diameter as backlight

Time-resolved Spectroscopy

- Observe emission at three horizontal positions with respect to plasma core (kernel): kernel (0 mm), 1.25 mm, and 2.5 mm

Argon

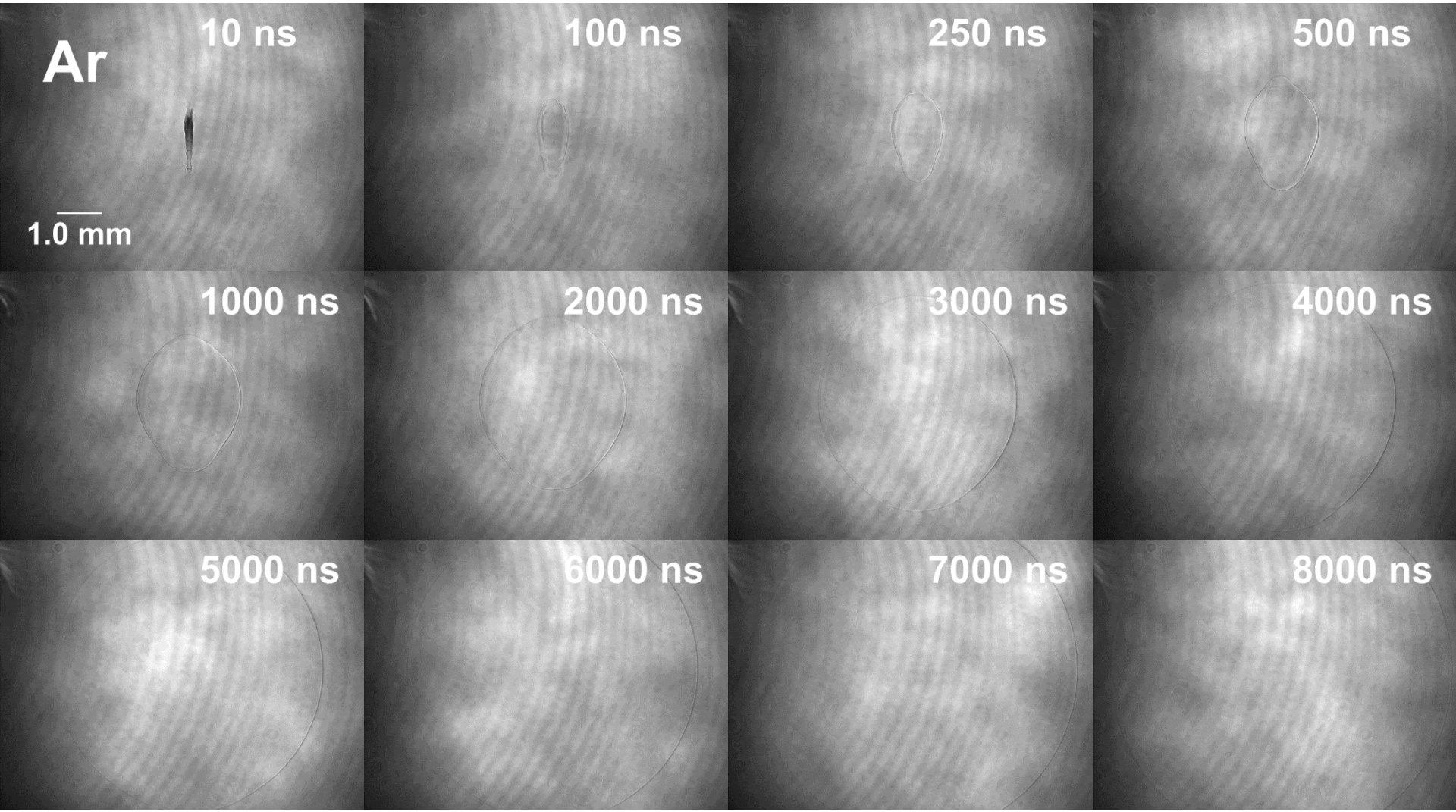
Ar
1.0 mm
10 ns
100 ns
250 ns
500 ns
1000 ns
2000 ns
3000 ns
4000 ns
5000 ns
6000 ns
7000 ns
8000 ns

Argon

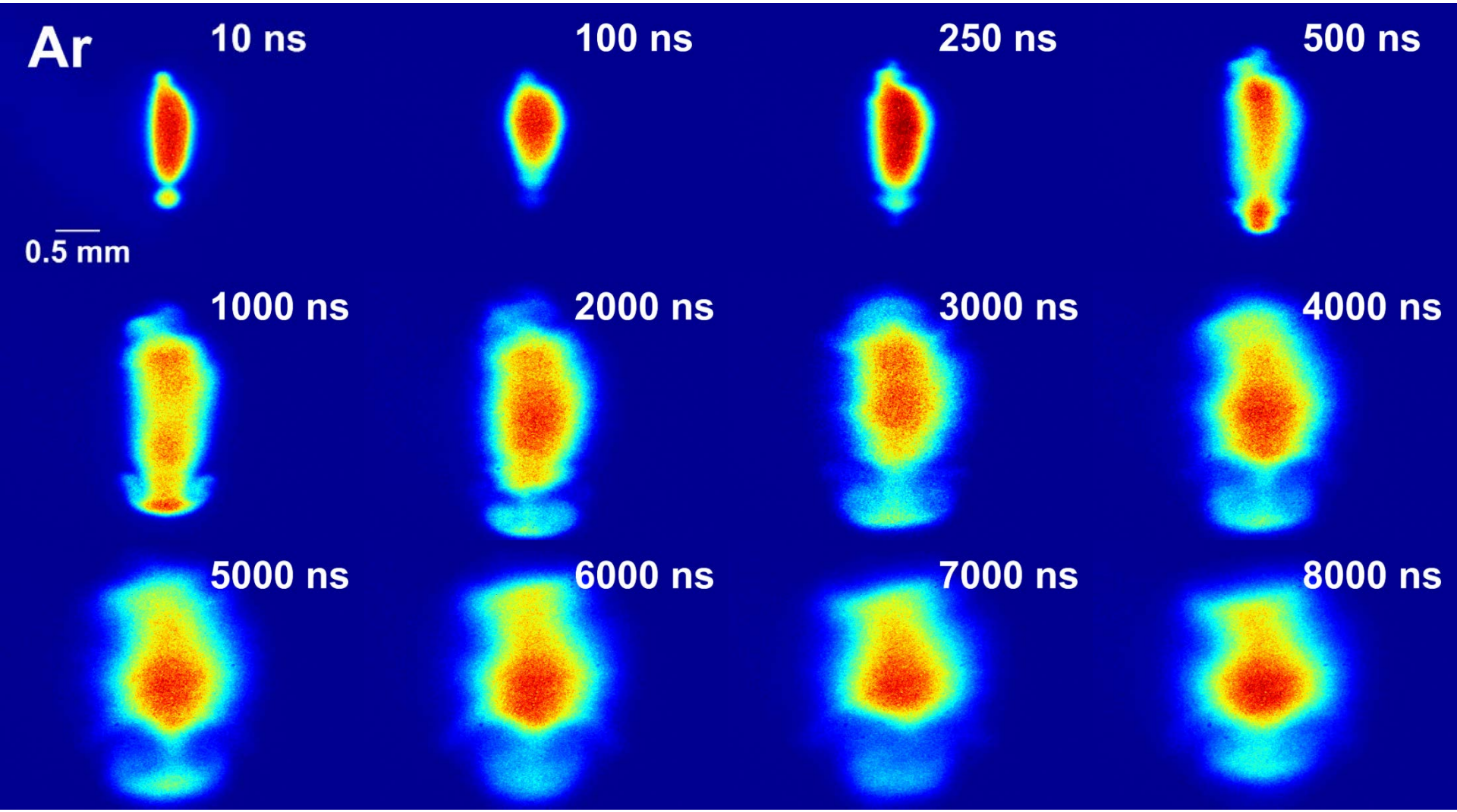
Ar
10 ns
100 ns
250 ns
500 ns
0.5 mm
1000 ns
2000 ns
3000 ns
4000 ns
5000 ns
6000 ns
7000 ns
8000 ns

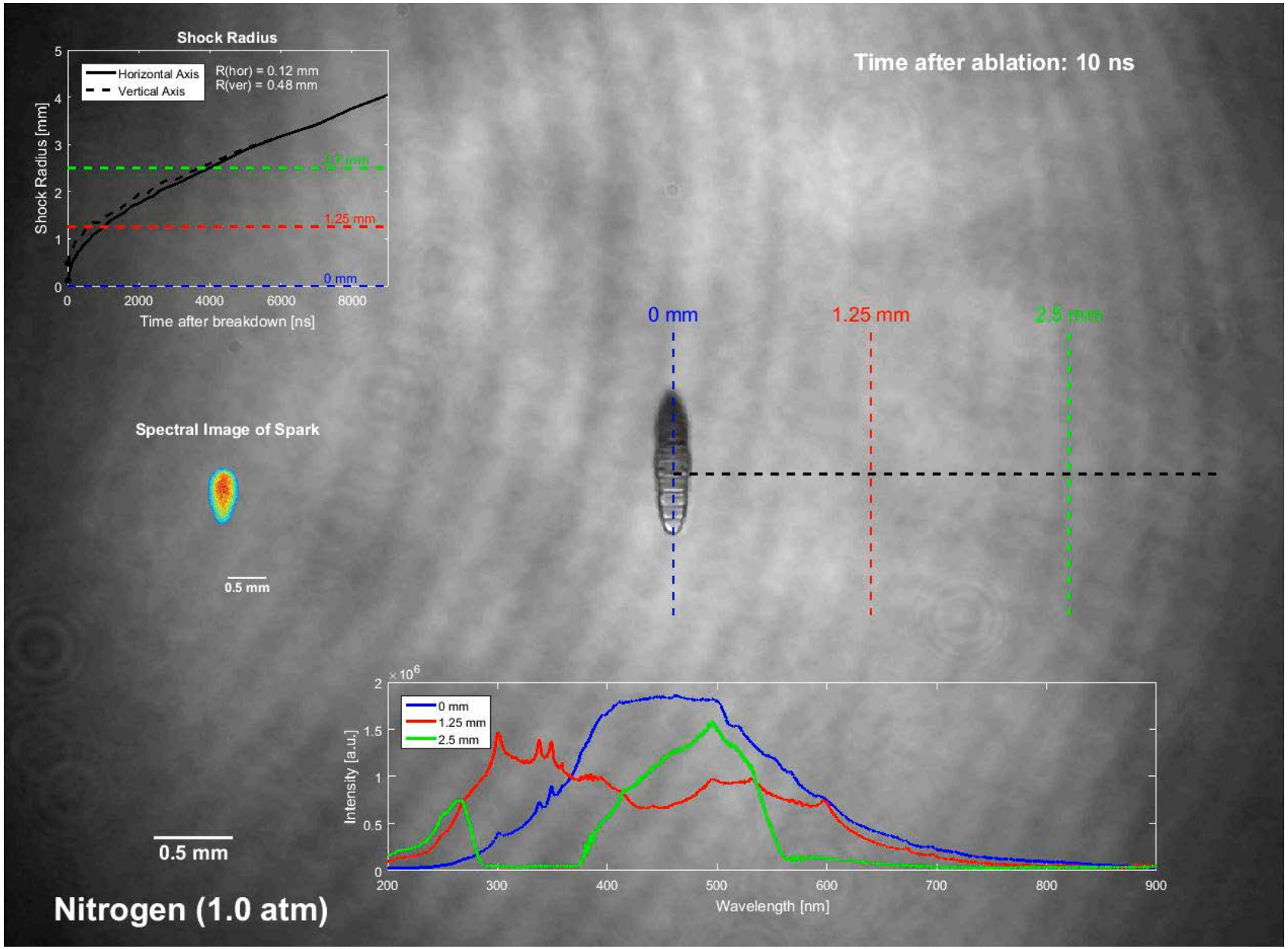
Shock Radius
Horizontal Axis
Vertical Axis
R(hor) = 0.12 mm
R(ver) = 0.48 mm
Shock Radius [mm]
Time after breakdown [ns]
2.5 mm
1.25 mm
0 mm
Time after ablation: 10 ns
0 mm
1.25 mm
2.5 mm
Spectral Image of Spark
0.5 mm
0.5 mm
Intensity [a.u.]
Wavelength [nm]
Nitrogen (1.0 atm)

Nitrogen

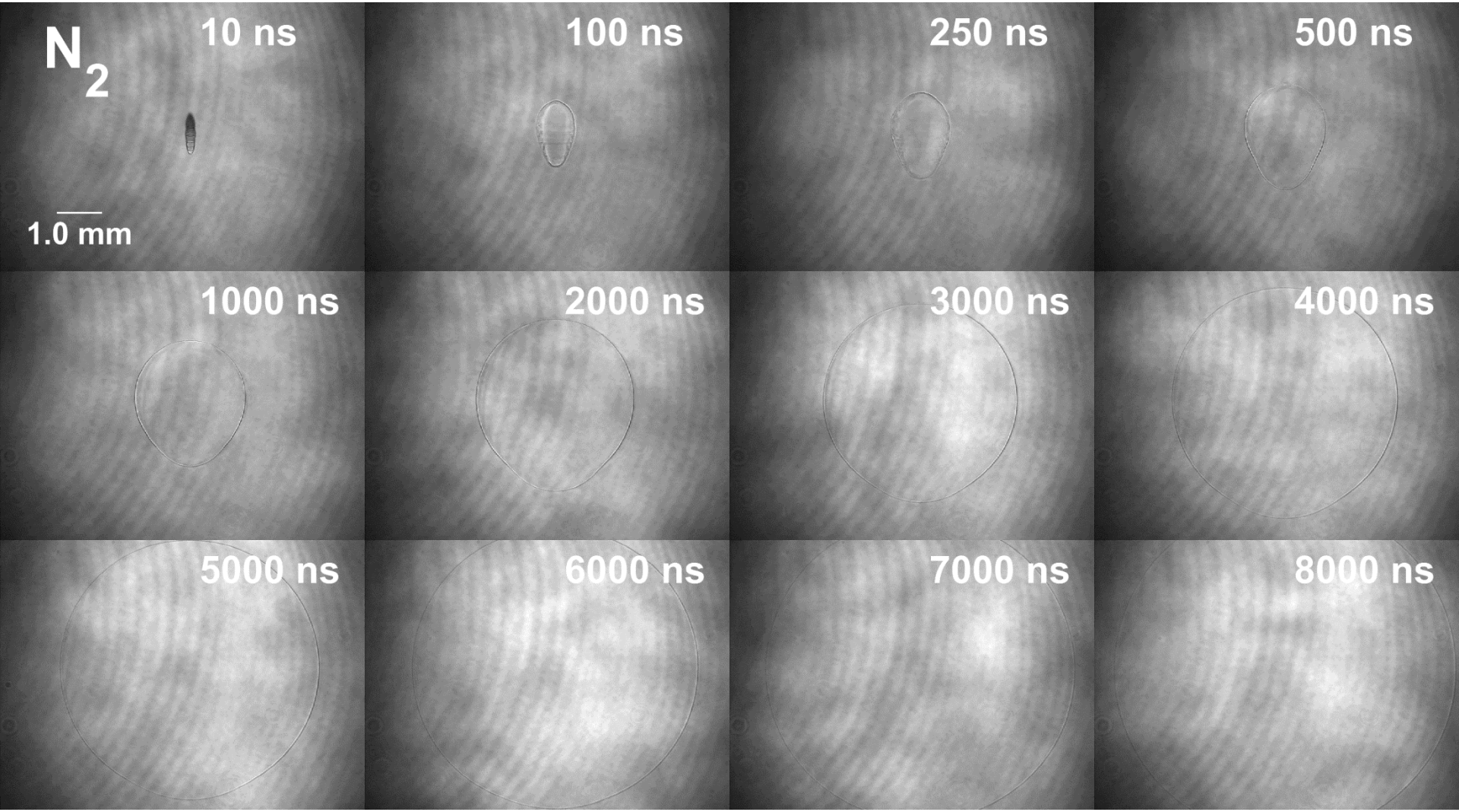
N_2
10 ns
100 ns
250 ns
500 ns
1.0 mm
1000 ns
2000 ns
3000 ns
4000 ns
5000 ns
6000 ns
7000 ns
8000 ns

Nitrogen

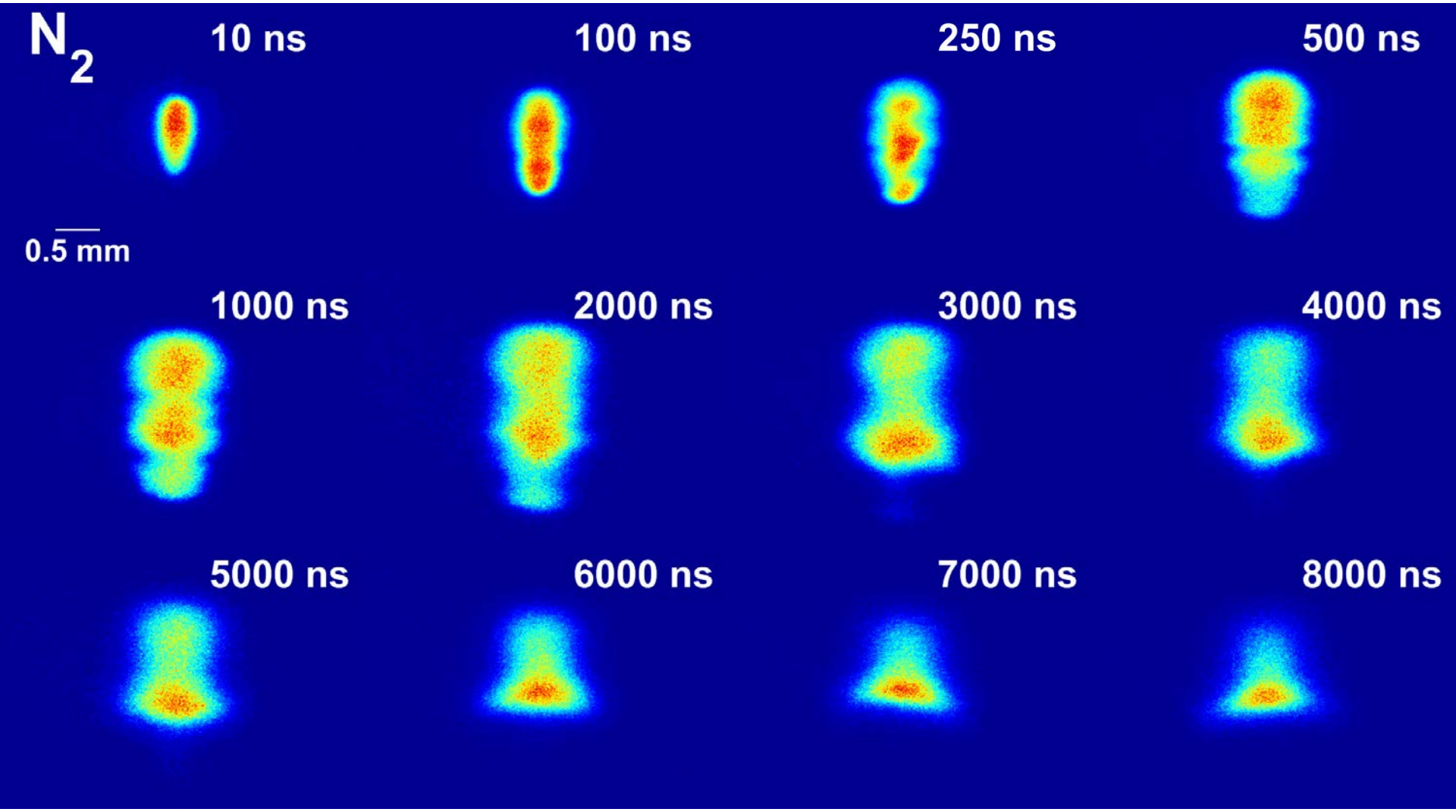
N_2
10 ns
100 ns
250 ns
500 ns
0.5 mm
1000 ns
2000 ns
3000 ns
4000 ns
5000 ns
6000 ns
7000 ns
8000 ns

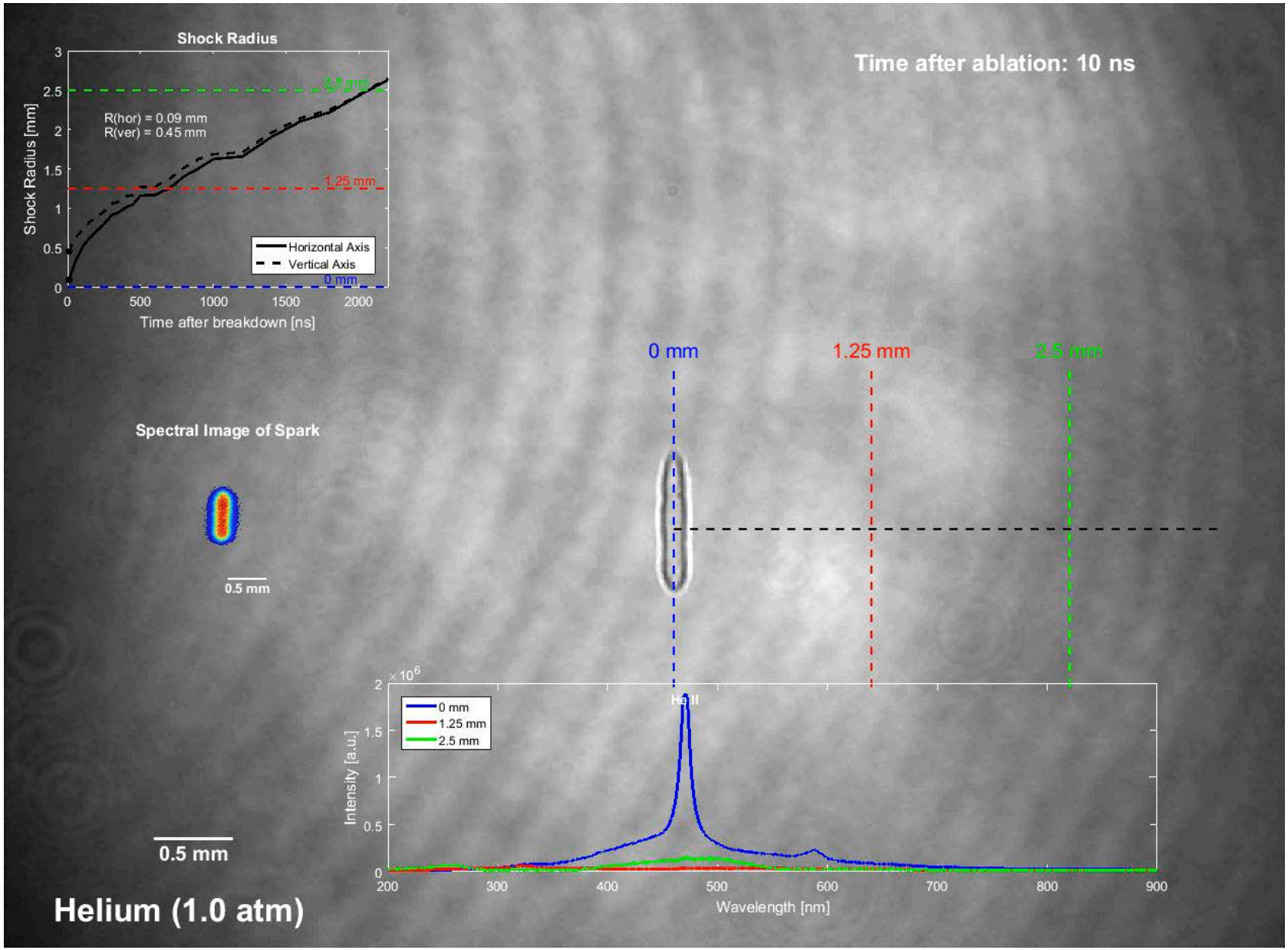
Shock Radius
Shock Radius [mm]
Time after breakdown [ns]
R(hor) = 0.09 mm
R(ver) = 0.45 mm
2.5 mm
1.25 mm
0 mm
Horizontal Axis
Vertical Axis
Time after ablation: 10 ns
0 mm
1.25 mm
2.5 mm
Spectral Image of Spark
0.5 mm
0.5 mm
Helium (1.0 atm)
He II
0 mm
1.25 mm
2.5 mm
Intensity [a.u.]
Wavelength [nm]

Helium

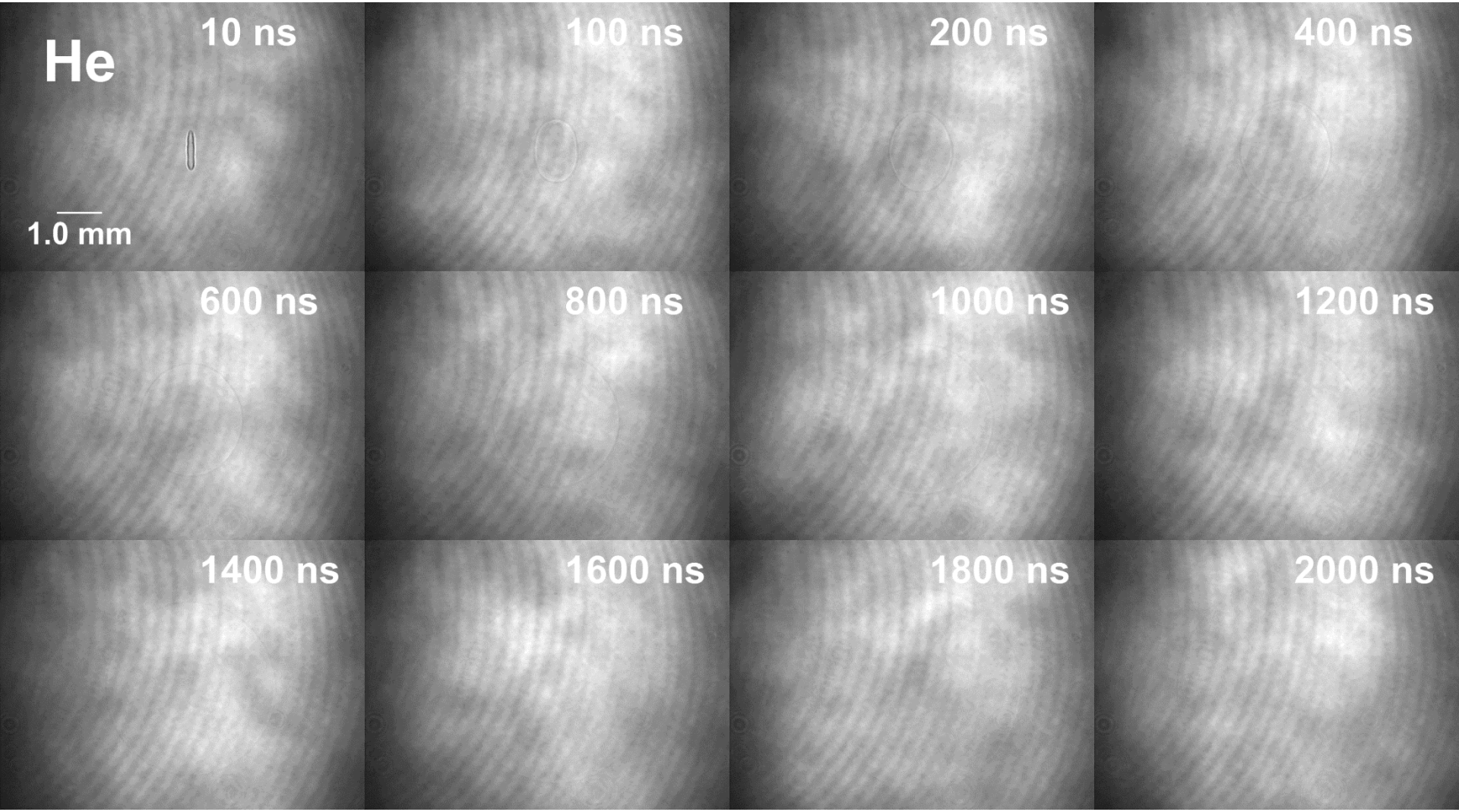
He
10 ns
100 ns
200 ns
400 ns
1.0 mm
600 ns
800 ns
1000 ns
1200 ns
1400 ns
1600 ns
1800 ns
2000 ns

Helium

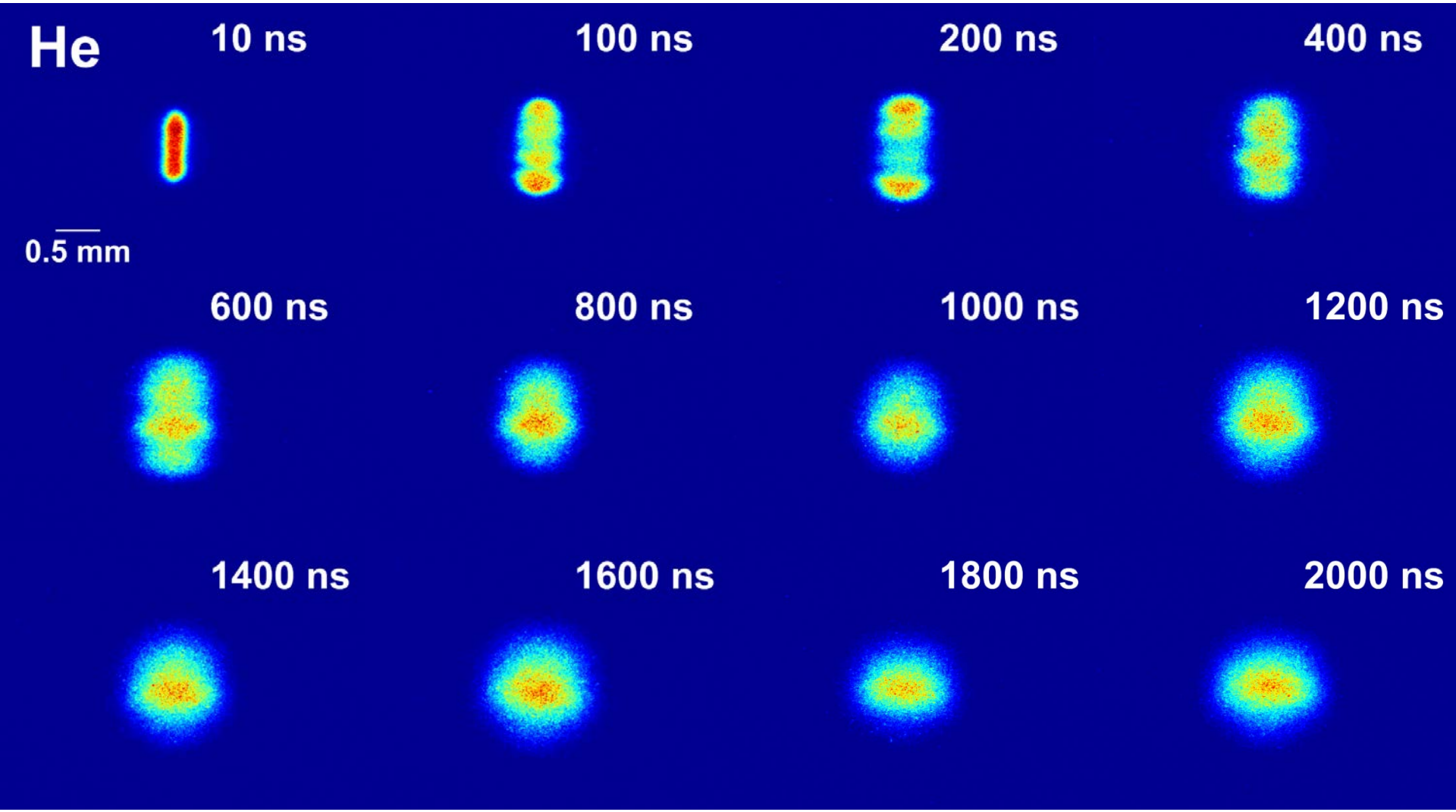
He
10 ns
100 ns
200 ns
400 ns
0.5 mm
600 ns
800 ns
1000 ns
1200 ns
1400 ns
1600 ns
1800 ns
2000 ns